ELSEVIER

Journal of Neuroscience Methods 170 (2008) 67–76

JOURNAL OF NEUROSCIENCE METHODS

www.elsevier.com/locate/jneumeth

Genetically encoded chloride indicator with improved sensitivity

Olga Markova [a,1], Marat Mukhtarov [a,1], Eleonore Real [b,2,3], Yves Jacob [b,2], Piotr Bregestovski [a,*]

[a] *Institut de Neurobiologie de la Méditerranée (INMED), INSERM U901, Parc Scientifique de Luminy, 13273 Marseille, France*

[b] *Unite of Genetics, Papillomavirus and Human Cancer, Department of Virology, Pasteur Institute, 25, rue du docteur Roux, 75724 Paris, France*

Received 11 September 2007; received in revised form 4 December 2007; accepted 22 December 2007

Abstract

Chloride (Cl) is the most abundant physiological anion. Abnormalities in Cl regulation are instrumental in the development of several important diseases including motor disorders and epilepsy. Because of difficulties in the spectroscopic measurement of Cl in live tissues there is little knowledge available regarding the mechanisms of regulation of intracellular Cl concentration. Several years ago, a CFP-YFP based ratiometric Cl indicator (Clomeleon) was introduced [Kuner, T., Augustine, G.J. A genetically encoded ratiometric indicator for chloride: capturing chloride transients in cultured hippocampal neurons. Neuron 2000; 27: 447–59]. This construct with relatively low sensitivity to Cl ($K_{app} \sim 160$ mM) allows ratiometric monitoring of Cl using fluorescence emission ratio. Here, we propose a new CFP-YFP-based construct (Cl-sensor) with relatively high sensitivity to Cl ($K_{app} \sim 30$ mM) due to triple YFP mutant. The construct also exhibits good pH sensitivity with pK_{α} ranging from 7.1 to 8.0 pH units at different Cl concentrations. Using Cl-sensor we determined non-invasively the distribution of $[Cl]_i$ in cultured CHO cells, in neurons of primary hippocampal cultures and in photoreceptors of rat retina. This genetically encoded indicator offers a means for monitoring Cl and pH under different physiological conditions and high-throughput screening of pharmacological agents.

Keywords: Fluorescent proteins; Real-time optical detection; Patch-clamp; Glycine receptor

1. Introduction

Chloride is the most abundant physiological anion. It is present in every cell in biological organisms and participates in a variety of physiological functions, such as regulation of cell volume, intracellular pH, fluid secretion and stabilisation of resting membrane potential (Aslanova et al., 2006; Pasantes-Morales et al., 2006; Suzuki et al., 2006). This ion is crucial for nervous system functioning. The main inhibitory drives in central and peripheral neuronal circuits are provided by GABAergic and glycinergic synapses, which operate through Cl-selective ionic channels (Bormann et al., 1987; Hamill et al., 1983). The concentration of intracellular Cl ($[Cl]_i$) and its permeance are highly regulated by a variety of Cl-selective channels and Cl transporters. Dysfunction of these proteins results in various diseases such as Bartter syndrome, startle disease, cystic fibrosis and epilepsy (Ashcroft, 2000; Lerche et al., 2005). Despite the importance of Cl for many cellular functions, there is little knowledge available on the mechanisms regulating Cl in either physiological or pathological conditions. This lack of information is primarily due to technical difficulties in the measurement of Cl flux in live cells.

Several methods have been proposed for monitoring $[Cl]_i$. Early approaches with Cl-selective microelectrodes showed that $[Cl]_i$ in some giant neurons of the snail *Helix aspersa* is low, about 8 mM (Neild and Thomas, 1974). This method has been used in several cell types, including astrocytes, mouse lacrimal acinar cells (Ozawa et al., 1988) and horizontal cells of the fish retina (Djamgoz and Laming, 1987). However, Cl-selective electrodes can only be reliably applied to relatively large cells.

Abbreviations: $[Cl]_i$, concentration of intracellular Cl; CFP, cyan fluorescent protein; CHO-K1, Chinese ovary cells; E_{Cl}, reversal potential for Cl; FRET, Fluorescence Resonance Energy Transfer; GFP, green fluorescent protein; GlyR, glycine receptor; HEK-293, human embryonic kidney cells; V_h, holding potential; YFP, yellow fluorescent protein.

* Corresponding author. Tel.: +33 4 91 82 81 19; fax: +33 4 91 82 81 01.
E-mail addresses: markova@inmed.univ-mrs.fr (O. Markova), mukhtarov@inmed.univ-mrs.fr (M. Mukhtarov), eleonorereal@yahoo.fr (E. Real), yjacob@pasteur.fr (Y. Jacob), pbreges@inmed.univ-mrs.fr (P. Bregestovski).
[1] Tel.: +33 4 91 82 81 18; fax: +33 4 91 82 81 01.
[2] Tel.: +33 1 45 68 87 53; fax: +33 1 45 68 89 66.
[3] Present address: Cold Spring Harbor Laboratory, Cold Spring Harbor, NY 11724, USA. Tel.: +1 516 367 8473; fax: +1 516 367 8372.

0165-0270/$ – see front matter © 2008 Elsevier B.V. All rights reserved.
doi:10.1016/j.jneumeth.2007.12.016

In addition, this method is slow and the preparation is time-consuming, and recordings are often distorted by the interference of the electrode with intracellular anions and anion leakage from the reference barrel.

The use of Cl-sensitive fluorescent dyes is a more convenient approach. Quinoline-based fluorescent dyes such as 6-methoxy-*N*-(3-sulphopropyl)quinolinium (SPQ), its derivative MQAE or 6-methoxy-*N*-ethylquinolinium chloride (MEQ) have been used for measurements of $[Cl]_i$ in a variety of preparations, including isolated growth cones, neurons, glia, different types of epithelial cells, fibroblasts and pancreatic beta-cells (see refs in Chub et al., 2006; Mansoura et al., 1999; Painter and Wang, 2006). Quinolinium compounds have low biological toxicity, relatively good sensitivity to and selectivity for Cl and a rapid response to changes in Cl. The major disadvantage of quinoline-based indicator dyes is that they are prone to a time-dependent decay in fluorescence because of the gradual leakage of dye from the labelled cells or bleaching (Biwersi and Verkman, 1991; Chub et al., 2006; Inglefield and Schwartz-Bloom, 1997; Krapf et al., 1988; Nakamura et al., 1997; Painter and Wang, 2006). Using these dyes needs either a short-interval exposure and a low acquisition rate (Schwartz and Yu, 1995) or recording images with two-photon scanning microscopy techniques (Marandi et al., 2002).

More recent approaches are based on using fluorescent proteins. It has been found that yellow fluorescent protein (YFP) is quenched by small anions and it can be used as a weak Cl-sensor (Wachter and Remington, 1999). Transgenic mice expressing YFP under the control of a potassium channel promoter were generated (Metzger et al., 2002) and were used for monitoring glutamate-induced elevations in $[Cl]_i$ (Slemmer et al., 2004).

The YFP-H148Q mutant, which has higher Cl sensitivity, has been proposed for monitoring changes in halide fluxes in cells (Jayaraman et al., 2000). This probe also exhibits good pH sensitivity (with apparent pK_α values from 7.0 to 8.0, depending on Cl concentration) and it has been shown to be a useful cellular halide indicator in various preparations (Jayaraman et al., 2000; Muanprasat et al., 2007; Pedemonte et al., 2005; Yang et al., 2003). A random mutagenesis approach allowed identification of two other mutations, I152L and V163S, which enhanced the protein sensitivity and accelerated its responses (Galietta et al., 2001a). These mutants have been successfully used for quantitative screening of CFTR chloride transport agonists (Galietta et al., 2001b; Rhoden et al., 2007) and for high-throughput screening of Cl-selective glycine and $GABA_A$ receptor channels (Kruger et al., 2005).

Further development of this approach has been achieved by construction of a fusion protein containing YFP combined with the Cl-insensitive cyan fluorescent protein (CFP). This construct allows fluorescence-resonance-energy-transfer (FRET)-based ratiometric measurements of $[Cl]_i$ in neurons (Kuner and Augustine, 2000). While this new indicator, termed Clomeleon, is excited by visible light, it shows little bleaching and it has been used for monitoring $[Cl]_i$ in transgenic animals (Duebel et al., 2006; Haverkamp et al., 2005). However, the sensitivity of this protein to Cl is low: the K_{app} is >160 mM. This is relatively far from the physiological range of $[Cl]_i$ in nervous systems of vertebrates, which is ~5–30 mM (Krapf et al., 1988; Rohrbough and Spitzer, 1996; Tyzio et al., 2006). Thus, development of molecules with sensitivities closer to this physiological range would provide a useful tool for monitoring $[Cl]_i$ in biological preparations.

In this study, we present a CFP-YFP-based construct with three mutations in YFP, which confer a high sensitivity to Cl (K_{app} ~30 mM). The construct also exhibits good pH sensitivity with pK_α ranging from 7.1 to 8.0 pH units at different Cl concentrations. This genetically encoded molecule is a sensitive probe for non-invasive monitoring of $[Cl]_i$ and pH under physiological conditions.

2. Material and methods

2.1. Cell cultures and transfection

The experiments were carried out on Chinese hamster ovary (CHO-K1) cell lines, on neurons of dissociated hippocampal culture and on slices from a retina of juvenile rats. Primary culture of neurons were prepared and maintained as described earlier (Fucile et al., 2000; Ivanov et al., 2006). CHO-K1 cells were obtained from the American type tissue culture collection (ATCC, Molsheim, France).

Two transfection protocols were used to deliver Cl-sensor cDNA into cultured cells. First, the Lipofectamine transfection protocol (Gibco, Invitrogen) with some modifications: briefly, cells were incubated in a solution containing 300 μl of Opti-MEM, 1 μl of Magnetofection CombiMag (OZ Bioscience, France), 6 μl of lipofectamine reagent 2000 (Invitrogen) and 1 μg of the Cl-sensor construct. After 30 min of incubation at 37 °C on a magnetic plate (OZ Bioscience, France) the transfection mixture was replaced with fresh complete growth medium supplemented in some experiments with 1 μM of strychnine (to prevent Cl influx through expressed GlyRs). In some experiments we used the second transfection protocol developed by OZ Bioscience (France): in brief, 1 μg cDNA was mixed with 1 μl of DreamFect Gold transfection reagent (OZ Bioscience) in 300 μl of OptiMEM (Invitrogen) and stored at room temperature for 30 min. The precipitate was added to the cells; 24–76 h after transfection, the cells were used in experiments.

2.2. Electroporation and slices preparation

For electroporation we used the protocol described previously (Matsuda and Cepko, 2004). Recording of fluorescent signals were carried out on retina slices from electroporated animals at the postnatal age P14–P15. Animals were anaesthetized with ether and killed by decapitation in agreement with the European directive 86/609/EEC requirements. Subsequently, the eye was enucleated and hemisected. After the vitreous body was removed, the pieces of retina were cut into 200 μm thick slices by a McILWAIN tissue chopper (The Mickle Laboratory Engineering Co. Ltd., England).

For monitoring Cl-sensor fluorescence, slices were placed in the chamber under the upright microscope (Axioskop, Zeiss, Germany) and were superfused (1.0–1.5 ml/min) with oxy-

genated solution containing (in mM): NaCl, 125; KCl, 3.5; $CaCl_2$, 2; $MgCl_2$, 1.3; NaH_2PO_4, 1.25; $NaHCO_3$, 26; and glucose, 10; equilibrated at pH 7.3 with 95% O_2 and 5% CO_2. The solution with elevated external K^+ concentration contained 40 mM KCl and 88.5 mM NaCl. For "low-Cl" external solutions NaCl and KCl salts were substituted with corresponding gluconate salts.

Prior to recording, slices were incubated at room temperature (22–25 °C) for at least one hour to allow recovery.

2.2.1. Calibration of pH dependence

For the calibration of Cl-sensor pH dependence in CHO cells the K^+/H^+ ionophore nigericin and the Cl/OH antiporter tributyltin chloride were used to equilibrate extra- and intracellular [Cl] and pH (Krapf et al., 1988; Marandi et al., 2002; Metzger et al., 2002; Trapp et al., 1996). In these experiments the external solution contained nigericin, 10 μM (Molecular Probes), tributultin chloride, 10 μM (Sigma), KCl/K-gluconate to a final concentration of K 140 mM and, in mM, $CaCl_2$, 2; $MgCl_2$, 2; glucose, 20; buffered by HEPES, 20 (adjusted with NaOH to different pH values). Solutions containing different concentrations of Cl were prepared by substituting equimolar concentrations of K-gluconate with KCl. Fluorescence spectra from 20 to 40 transfected CHO cells were registered for each pH and Cl. Results are expressed as mean ± S.D.

2.3. Electrophysiological recordings

Whole-cell recordings were conducted using an EPC-9 amplifier (HEKA Elektronik, Germany) at room temperature (~20–25 °C). Cells were continuously superfused with external solution through an independent tube. The external solution contained (mM): NaCl 140, $CaCl_2$ 2, KCl 2.8, $MgCl_2$ 2, HEPES 20, glucose 10; pH 7.3; 315 mOsm. The patch pipette solution contained (mM): KCl (0–150) or K-gluconate (0–150); $MgCl_2$ 2; MgATP 2, HEPES/KOH 20, BAPTA 1; pH 7.3; 290 mOsm. To vary the Cl concentration from 0 to 150 mM, a combination of K-gluconate and KCl at a constant K^+ concentration were used. Pipettes were pulled from borosilicate glass capillaries (Harvard Apparatus Ltd, USA) and had resistances of 5–7 MΩ.

In some experiments perforated-patch recordings were performed using gramicidin-containing intracellular solution. The small pores formed by gramicidin are selectively permeable to monovalent cations but not permeable to Cl (Myers and Haydon, 1972). Gramicidin was added to the pipette solution to a final concentration of 80–100 μg/ml immediately before use. Glycine was applied locally from pipettes using pressure pulses with "Picospritzer" (General Valve Corporation, USA). The pipettes were filled with an external solution containing 1 mM glycine and were placed 50–100 μm from the soma of the cells. Depending on the purpose of experiment, the duration of pressure applications varied from 10 ms to several minutes.

To measure the Cl reversal potential (E_{Cl}), the current–voltage (*I–V*) relations of responses to glycine were recorded. Voltage ramps (from −70 to +30 mV or from −60 to +40 mV, duration 100 ms) were applied before and during agonist application. The net *I–V* relations of glycine-activated currents were obtained by digital subtraction of the ramp current in the absence of agonist from that obtained during agonist application. $[Cl]_i$ values were calculated using the Nernst equation ($E_{Cl} = -58 \log([Cl]_i/[Cl]_o)$).

2.4. Real-time fluorescence imaging

Fluorescence images were acquired using a customized digital imaging microscope. Excitation of cells at various wavelengths was achieved using a 1 nm bandwidth polychromatic light selector equipped with a 100 W xenon lamp (Polychrome II; Till Photonics, Germany). The light intensity was attenuated using neutral density filters. A dichroic mirror (495 nm; Omega Optics, USA) was used to deflect light onto the samples. Fluorescence was visualized using an upright microscope (Axioskop, Zeiss, Germany) equipped with an infinity-corrected 60× water-immersion objective (n.a. = 0.9; LumPlanFL; Olympus, USA). Fluorescent emission light passed to a 12-bit charge-coupled device digital camera system equipped with image intensifier (PentaMax 512EEV-GENIV; Princeton Instruments, USA). Images were acquired on a computer via a DMA serial transfer. All peripheral hardware control, image acquisition and image processing were achieved using customized routines inside MetaFluor software (International Imaging, USA). The average fluorescence intensity of each region of interest (ROI) was measured. The mean background fluorescence (measured from a non-fluorescent area) was subtracted and the complete spectra, and/or the intensity ratios (F_{480}/F_{440}), were determined.

3. Results

3.1. Structure of Cl-sensor construct

The Cl-sensor construct presented in this study, similarly to Clomeleon (Kuner and Augustine, 2000), is based on the coupling of CFP with YFP via a peptide linker (Fig. 1A, Appendix B Supplementary 1). In order to enhance the sensitivity of YFP to halide, three missense mutations (Galietta et al., 2001a) were introduced using two sets of oligonucleotides encoding for the amino acid substitution H148 → Q, I152 → L and V163 → S, and eYFP 5′ and 3′ terminus-specific short degenerate primers introducing respectively Bgl II and BamH I restriction sites for easy cloning.

To facilitate the autonomous folding of the two fluorescent proteins (CFP and mutated eYFP) and keep a distance between them compatible with a FRET application, an adapter encoding for a peptide linker was introduced in the polylinker of the eCFP expression plasmid eCFP-C1 (Clontech), between the BspE I and BamH I restriction sites. The adapter generated by the annealing of two complementary oligonucleotides encodes for the following peptidic sequence: GSGSGENLYFAGGGSGGSGS. The Cl-sensor expressing plasmid was finalized by ligating in frame at the BamH I restriction site of the linker the Bgl II–BamH I DNA fragment encoding for the mutated eYFP.

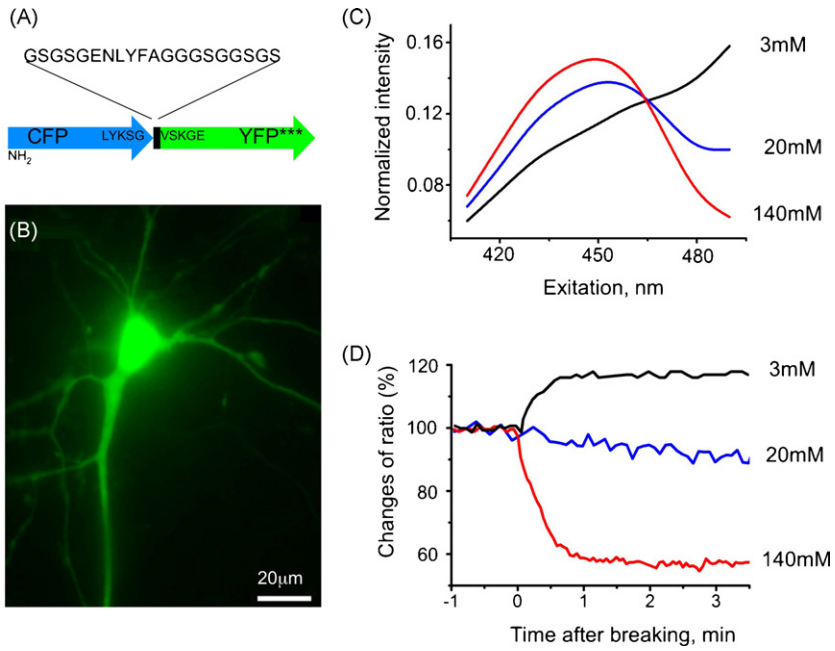

Fig. 1. Design and fluorescence properties of Cl-sensor. (A) Schematic representation of Cl-sensor construct; *** indicates three mutations: YFP-H148Q, -I152L and -V163S in the YFP sequence. (B) Image of a hippocampal neuron expressing Cl-sensor. Neurons were transfected with lipofectamine and the image was obtained 24 h after transfection. (C) Normalized spectra of Cl-sensor. Whole-cell recording from CHO cells with pipettes containing different Cl concentrations (shown in the graph). Note that spectra have a common point at 465 nm. (D) Changes in the fluorescence ratios (F_{480}/F_{440}) after whole-cell penetrations with pipettes containing different Cl concentrations (shown in the graph). Culture of CHO cells, 24–48 h after transfection.

3.2. Main properties of Cl-sensor

For *in vivo* analysis Cl-sensor was transiently expressed in CHO and HEK cells and in neurons of dissociated hippocampal culture, using lipofectamine transfection. Expression was already observable 12 h after transfection and remained at high levels for at least 4 days. The Cl-sensor fluorescence was distributed homogeneously throughout neurons with no preferential staining of membrane or intracellular organelles (Fig. 1B).

For estimation of the fluorescence spectral properties of Cl-sensor and for its calibration, simultaneous monitoring of fluorescence signals and whole-cell recordings with different Cl concentrations in the pipette solution (from 0 to 150 mM) performed. The excitation spectra (from 410 to 490) were recorded and for convenience of analysis each of them was normalized (see Supplementary 2). At high (140 mM) internal Cl concentration, normalized spectra showed a maximal peak at ~450 nm with a close to minimum at ~490 nm. Lowering the Cl concentration in the pipette solutions resulted in elevation of normalized fluorescence intensity at 480 nm and its reduction at 440–450 nm (Fig. 1C). We found that normalized spectra had a common point near 465 nm (Fig. 1C). For every spectrum the intensity at this point was Cl-independent. Thus, our Cl-sensor with triple-mutated YFP can be used as a ratiometric excitation wavelength indicator.

For ratiometric monitoring, excitation wavelengths 480 and 440 nm were selected, as this ratio ($R = F_{480}/F_{440}$) possesses good resolution. The duration of excitation at each wavelength was usually 10–20 ms, so acquisition of one ratiometric point took 20–40 ms. Fig. 1D illustrates changes in R in whole-cell recordings from three cells, using pipettes with solutions containing different Cl concentrations. Obtaining the whole-cell configuration by rupturing the membrane with a pipette containing 140 mM Cl resulted in a strong decrease in R. Fluorescence reached a steady-state level in ~1 min, reflecting the time for cytoplasmic Cl equilibration with that in the pipette solution. In contrast, on rupture of the membrane with the pipette containing 3 mM Cl an increase in R was observed. Transition to the whole-cell configuration with a pipette containing 20 mM Cl did not produce a significant change in R, reflecting the fact that in the recorded cell this value is close to the native concentration of Cl in cytoplasm (Fig. 1D). Importantly, using 3 mM Cl in the pipette solution resulted in an ~20% change in R in comparison with 20 mM. This high dynamic range provides the basis for reliable monitoring of Cl at physiological intracellular concentrations.

The calibration curve shown in Fig. 2 confirms the high sensitivity of Cl-sensor to Cl. This curve was obtained with simultaneous monitoring of fluorescence and whole-cell recording, and it represents the dependence of $R = F_{480}/F_{440}$ on the Cl concentration in the pipette. In different cells pipettes containing intracellular solutions with Cl concentrations from 0 to 150 mM were used (pH 7.3). Each point is the mean value from 4 to 6 cells. From this dependence, the estimated change in concentration of Cl causing a 50% change in the fluorescence ratio (K_{app}) was 28 ± 5 mM.

This *in vivo* analysis demonstrates that Cl-sensor exhibits a more than five-fold higher sensitivity to Cl than Clomeleon ($K_{app} > 160$ mM) (Kuner and Augustine, 2000) and provides the possibility of ratiometric monitoring with alternating excitation wavelengths. This last feature allows rapid ratiometric acquisi-

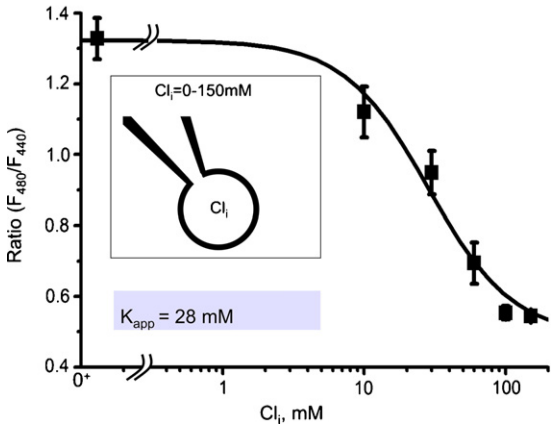

Fig. 2. Calibration of Cl-sensor. The relationships between fluorescence excitation ratio (F_{480}/F_{440}) and $[Cl]_i$ obtained from whole-cell recordings with pipettes containing solutions with different Cl concentrations (from 0 to 150 mM). Each data point represents the mean ± SEM from 4 to 6 cells. The error bars that are invisible are smaller than the symbols. The K_{app} value (50% fluorescence change) was 28 ± 5 mM (mean from the sigmoidal fit). Culture of CHO cells, 24–72 h after transfection.

tion and it is particularly valuable when using imaging setups equipped with polychromatic devices.

3.3. pH Sensitivity of Cl-sensor

It is well documented that the GFP family of fluorescent proteins exhibits significant pH dependence over a broad range of pH values (Elsliger et al., 1999; Jayaraman et al., 2000; Kneen et al., 1998; Kuner and Augustine, 2000; Llopis et al., 1998; Metzger et al., 2002). We examined the sensitivity of Cl-sensor to pH using the "nigericin-tributyltin" equilibrating protocol, which allows minimization of the transmembrane pH and Cl gradients (Marandi et al., 2002; Metzger et al., 2002; Rhoden et al., 2007; Trapp et al., 1996; Verkman, 1990).

The effect of pH alterations was examined in CHO cells transfected with Cl-sensor. The application of the solutions containing nigericin and tributyltin caused changes in the fluorescence ratio following pH alteration in the range 5.5–10. Fig. 3 shows a representative trace of fluorescence ratio (480/440 nm) changes over the pH range 6–10 (Fig. 3A) and steady-state fluorescence pH titration curves of Cl-sensor in solutions containing different Cl concentrations (Fig. 3B). The dependencies are fitted well by the standard dose-response equation with a Hill coefficient of ~0.9. Apparent pK_α values increased with elevation of Cl concentration and varied from 7.1 to 8.0 over the Cl concentration range 4–140 mM. These results demonstrate that Cl-sensor also exhibits a relatively high sensitivity to pH changes in physiological conditions. This range of pK_α alterations is similar to those obtained for YFP-H148Q or YFP-H148Q/I152L proteins (Jayaraman et al., 2000; Rhoden et al., 2007).

3.4. Modulation of intracellular Cl at activation of glycine receptor channels

With further analysis we established how changes in Cl-sensor fluorescence would accompany manipulations designed

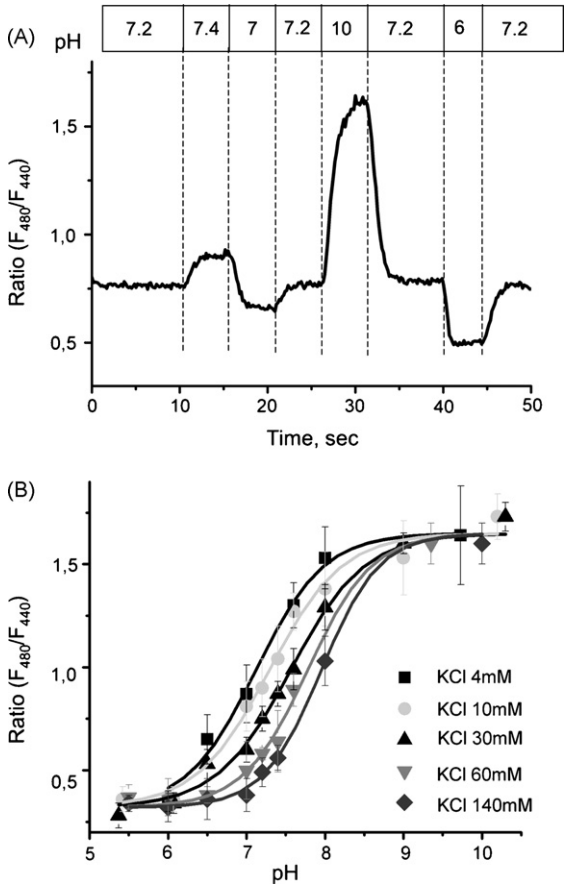

Fig. 3. pH Sensitivity of Cl-sensor. (A) Representative trace of the fluorescence ratio changes with variation of pH in the range 6–10 pH units. CHO cells, 48 h after transfection with Cl-sensor cDNA. The "nigericin-tributyltin" equilibrating solution contained 30 mM Cl. The pH values are shown above the trace. (B) Titration of Cl-sensor fluorescence ratio as a function of pH at different Cl concentrations in CHO cells. Each point presents a mean of 15–42 cells ± S.D. A sigmoidal curve was fitted to the data points to calculate the apparent pK_α. For solutions containing KCl 4 mM, 10 mM, 30 mM, 60 mM and 140 mM, corresponding pK_α were 7.1, - 7.3, - 7.5, - 7.8 and – 8.0, respectively.

to alter $[Cl]_i$ on activation of Cl-selective glycine receptor (GlyR) channels. CHO cells were co-transfected with Cl-sensor and human α1 GlyR, and simultaneous monitoring of fluorescence signals and whole-cell ionic currents were performed.

In transfected cells, application of 1 mM glycine caused slowly desensitizing currents whose amplitude varied depending on the holding potential (V_h) (Fig. 4A). Corresponding fluorescence also varied (Fig. 4B), indicating that $[Cl]_i$ was well regulated by the holding potential. To determine the reversal potential for Cl (E_{Cl}), a ramp protocol (deflections in the Fig. 4A, see Section 2 (Methods)) was used during steady-state currents at different values of V_h. $[Cl]_i$ was calculated from E_{Cl} using the Nernst equation. In the example presented, changes in membrane potential from −70 mV to +20 mV with permanent activation of GlyR channels resulted in a shift in E_{Cl} by ~60 mV (Fig. 4C), which corresponds to an ~10-fold change in $[Cl]_i$. In this set of experiments, also with using the gramicidin perforated-patch configuration, a similar shift in E_{Cl} was observed in the other 19 cells.

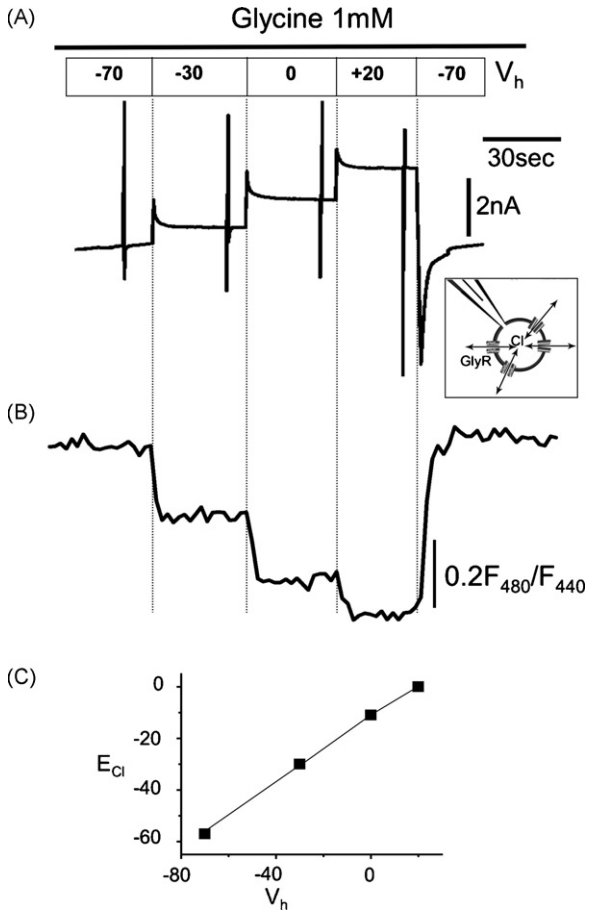

Fig. 4. Estimation of $[Cl]_i$ changes induced by activation of Cl-selective glycine receptor channels. (A, B) Simultaneous recordings of glycine-induced whole-cell currents (A) and F_{480}/F_{440} fluorescence ratio (B) on changing the V_h from −70 mV to +20 mV in a CHO cell co-transfected with cDNA of Cl-Sensor and the human α1 GlyR subunit. The recording pipette contained 3 mM Cl. The duration of glycine (1 mM) application is shown by the bar at the top. Changes in V_h are indicated by labelled rectangles above the current traces. Vertical deflections in (A) represent the current deflections in response to voltage ramp application. Insert below the current trace illustrates the scheme of recording. (C) Plot of E_{Cl} dependence on changes in V_h at continuous glycine application. Shifts in E_{Cl} were obtained with a ramp protocol. The same cell as in A,B. Note that, due to Cl influx through GlyR channels, E_{Cl} at different values of V_h changed from about –60 to 0 mV. Estimated $[Cl]_i$ for different E_{Cl} were: 13 mM, 43 mM, 95 mM and 140 mM.

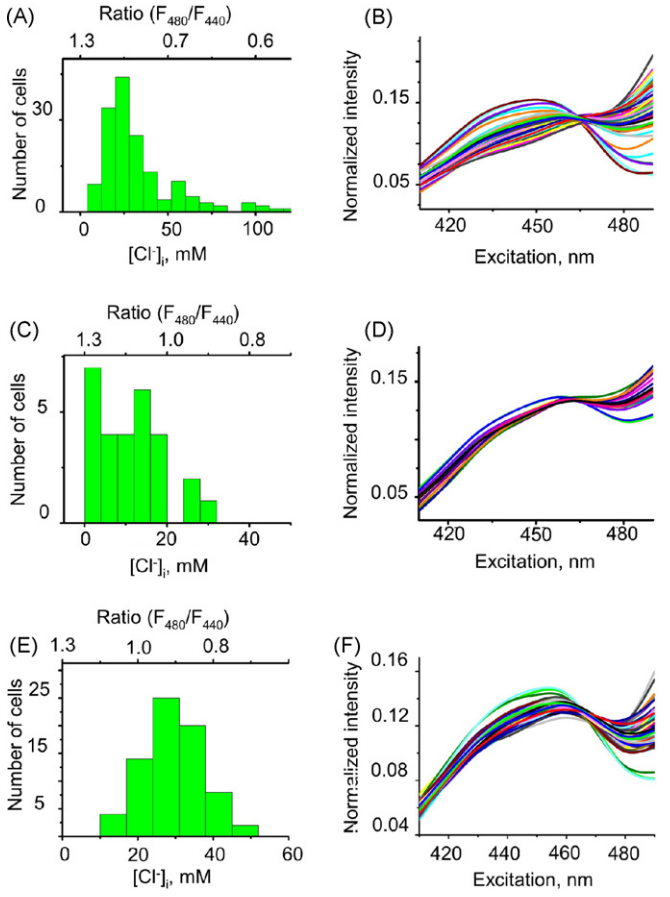

Fig. 5. Non-invasive estimation of $[Cl]_i$ in CHO cells, hippocampal neurons and in photoreceptors from a rat retina slices. (A) Histogram of $[Cl]_i$ distribution in CHO cells ($n = 200$) measured non-invasively with Cl-sensor. Ratios F_{480}/F_{440} (top abscissa) were calculated from spectra presented in B. The values for Cl (bottom abscissa) were taken from the calibration curve (Fig. 2). The distribution of $[Cl]_i$ was a good fit to a Gaussian curve with a mean of 23 ± 9 mM ($n = 200$). (B) Family of normalized fluorescence spectra of Cl-sensor in different CHO cells. Spectrum for each cell is shown by different colour. (C) Histogram of $[Cl]_i$ distribution in hippocampal neurons measured non-invasively with Cl-sensor. The mean $[Cl]_i = 11 \pm 2$ mM ($n = 33$). Dissociated culture of hippocampus, eight DIV. (D) Family of normalized fluorescence spectra of Cl-sensor in different hippocampal neurons presented in (C). (E) Histogram of $[Cl]_i$ distribution in photoreceptor cells from a P15 rat retina slices measured non-invasively with Cl-sensor. In comparison with CHO cells and hippocampal neurons, the distribution of $[Cl]_i$ in neurons is shifted to higher concentrations with a mean of 31 ± 9 mM ($n = 76$). The values for Cl were taken from the calibration curve (Fig. 2). (F) Family of normalized fluorescence spectra of Cl-sensor in different photoreceptor cells presented in (E).

These results demonstrate that activation of GlyR channels can rapidly and strongly modify $[Cl]_i$, supporting previous observations that $[Cl]_i$ is a highly dynamic parameter depending on the activity of Cl-selective channels or Cl transporters in normal and pathological conditions (Haverkamp et al., 2005; Khalilov et al., 2003; Rohrbough and Spitzer, 1996; Tyzio et al., 2006).

3.5. Non-invasive estimation of intracellular Cl in CHO cells and in hippocampal neurons

We used Cl-sensor for non-invasive estimation of $[Cl]_i$ in CHO cells, in hippocampal neurons and in photoreceptors from slices of rat retina. The spectra of transfected cells were measured and ratios (F_{480}/F_{440}) were calculated.

Fig. 5A illustrates the distribution of $[Cl]_i$ in 200 CHO cells expressing Cl-sensor. This histogram was obtained from excitation spectra, determined for each cell (Fig. 5B) and the calibration curve (Fig. 2). The distribution represents a good fit to a Gaussian curve with a mean of 23 ± 13 mM ($n = 200$).

Similar analysis was performed on cultured hippocampal neurons transfected with Cl-sensor (Fig. 5C and D). Estimated non-invasively, $[Cl]_i$ in soma of hippocampal neurons varied for different cells mainly in the range 3–24 mM with a mean value of 11 ± 2 mM ($n = 33$).

3.6. Non-invasive monitoring of intracellular Cl in retinal cells

We developed also the strategy for non-invasive monitoring of $[Cl]_i$ in brain slices. For this Cl-sensor cDNA was delivered in retina of neonatal rats using electroporation protocol (Matsuda and Cepko, 2004). For fluorescent analysis slices of retina (200 μm) were prepared from electroporated animals at the age P14-P15. The expression of fluorescent proteins was observed in a wide area with particularly massive fluorescence in photoreceptor layer. Some cells from inner nuclear layer (amacrine and bipolar cells) also exhibited robust expression of fluorescent proteins (not shown).

For non-invasive estimation of $[Cl]_i$ we primary used photoreceptor cells expressing Cl-sensor. Fluorescent spectra were recorded (Fig. 5F) and $[Cl]_i$ was calculated. As illustrated in Fig. 5E, the level of $[Cl]_i$ strongly varied (from 10 to 50 mM). In photoreceptor cells from a P15 rat retina slices the mean $[Cl]_i$ value was 31 ± 9 mM ($n = 76$), which is significantly higher than in hippocampal neurons and in CHO cells.

3.7. Potassium-induced depolarization

In different preparations, depolarization of cells was shown to induce a fall in intracellular pH (Willoughby and Schwiening, 2002; rev. Chesler, 2003) and an increase in Cl (Slemmer et al., 2004). We analysed the ability of Cl-sensor to monitor the functional responses to depolarization of photoreceptor cells in slices of retina. To induce depolarization, an external solution containing 40 mM K^+ was bath-applied to retina slices from P14–P15 rats. Fluorescence ratios (F_{480}/F_{440}) were monitored at a low acquisition rate (0.1 Hz).

To distinguish whether changes in the fluorescence ratio with K^+-induced depolarization are caused predominantly by elevation of $[Cl]_i$ or by acidification, responses to high K^+ were recorded in an external solution containing normal Cl concentration (135 mM) and then in a "low-Cl" solution containing only 6.5 mM Cl (substitution with gluconate).

As illustrate Fig. 6A, in normal Cl-containing external solution, K^+-induced depolarization caused changes in the fluorescence ratio corresponding an increase in $[Cl]_i$ of ~35 mM. This increase was strongly and reversibly suppressed in the "low-Cl" solution. On average, in normal Cl-containing solution, depolarization induced by application of 40 mM K^+ caused an elevation in $[Cl]_i$ of 44 ± 4 mM ($n = 5$, Fig. 6B). In the "low-Cl" solution this increase was 5 ± 1 mM (Fig. 6B). The base level of $[Cl]_i$ before depolarization was 37 ± 6 mM ($n = 5$), indicating that in photoreceptors application of 40 mM K^+ caused an elevation of $[Cl]_i$ to more than 70 mM. These results agree with recent observations on neurons in primary hippocampal cell culture following glutamate-induced depolarization (Slemmer et al., 2004) and suggest that, monitored with Cl-sensor, changes in fluorescence ratio with K^+-induced depolarization mainly represent elevation of $[Cl]_i$ in photoreceptors of retinal slices.

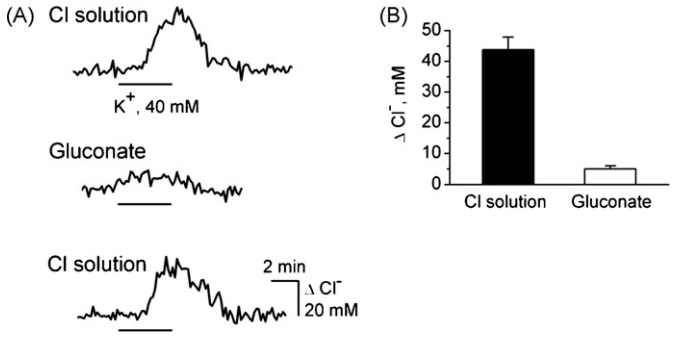

Fig. 6. Non-invasive monitoring of $[Cl]_i$ changes in retinal cells induced by depolarization. (A) Example of $[Cl]_i$ changes in response to 40 mM K^+-induced depolarization in solutions containing 135 mM Cl (top and bottom traces) and 6.5 mM Cl (middle trace). Photoreceptor cell from a P15 rat retina slice. "High-K^+" solution was bath-applied. (B) Average changes in $[Cl]_i$ following "high-K^+"-induced depolarization in normal (black column) and "low-Cl^-" (white column) solutions. Data are means ± SEM of 5 photoreceptor cells. The base level of $[Cl]_i$ before depolarization was 37 ± 6 mM ($n = 5$).

4. Discussion

Genetically encoded fluorescent optical probes have become powerful tools for visualisation of ions and proteins in live cells (Demaurex and Frieden, 2003; Gandhi et al., 2000; Gorostiza et al., 2007; Miyawaki, 2003; Siegel and Isacoff, 1997). In this study we present genetically encoded indicator for the spectroscopic monitoring of intracellular Cl with improved sensitivity. The Cl-sensor consists of CFP and mutated YFP connected by a linker. Its construction is similar to that of the analogous protein Clomeleon (Kuner and Augustine, 2000) but, due to mutations in the YFP, our Cl-sensor exhibits ~5-fold higher sensitivity to Cl with K_{app} ~30 mM. As in mammalian nervous system the physiological range of $[Cl]_i$ is, in general, in the range ~5–30 mM (Krapf et al., 1988; Rohrbough and Spitzer, 1996; Tyzio et al., 2006), this probe may be a useful tool for monitoring distribution and changes in intracellular Cl in various biological preparations.

The Cl-sensor also allows ratiometric monitoring at alternating excitation wavelengths. A significant limitation in the use of Cl indicators has been the lack of a Cl-dependent change in spectral shape, which precludes ratiometric measurements. Synthesis of series of dual-wavelength Cl-sensitive fluorescent indicators has overcome this limitation (Jayaraman et al., 1999). However, the delivery of these organic compounds into cells, and their toxicity, as well as difficulties in specific conjugation of chemical compounds with proteins, greatly limit their use for specific targeting in cellular compartments. The genetically encoded protein Clomeleon (Kuner and Augustine, 2000) overcomes these limitations. It serves as an emission ratiometric indicator (F_{527}/F_{485}) based on FRET between the fluorophores of CFP and YFP. This makes it possible to determine $[Cl]_i$ by monitoring the fluorescence emission ratio. Our results show that CFP–YFP-linked constructs can also be used as excitation ratiometric indicators. This feature allows high-speed recordings using conventional setups with, for instance, Polychrome (Till Photonics, Germany) or other devices for a rapid change of excitation wavelength.

Similarly to other fluorescent proteins from the GFP family, Cl-sensor exhibits a relatively high sensitivity to pH variations. Suppression of YFP fluorescence by Cl or other halides is due to protonation of the chromophore (Wachter et al., 2000) and it alters the electrostatic environment producing a change in apparent pK_α (Jayaraman et al., 2000.). It is, therefore, possible that treatments resulting in a change of pH_i may alter the responses of YFP-based probes. We estimated that Cl-sensor exhibits a relatively high sensitivity to pH changes in physiological conditions. In the pH range 6.8–7.8 a shift of 0.1 pH units resulted in change in the ratio F_{480}/F_{440} of ~0.05 units, i.e., by at most 6% of the whole dynamic range of the probe.

It is well documented that changes in H^+ concentration can transiently occur in extra and intracellular compartments of neurons and glia in response to cell activation by neurotransmitters or other factors (revs. Chesler, 2003; Deitmer and Rose, 1996). In Purkinje cells, depolarization-induced action potential firing for 10 s caused pronounced acidification in dendrites (the average was 0.11 pH units) but rather negligible acidification (0.03 pH units) in soma (Willoughby and Schwiening, 2002). In cultured hippocampal neurons, glutamate application induced an acidification of about 0.2 pH units (Slemmer et al., 2004). From the calibration graphs we estimate that, at this range of pH modulation (0.2 units), using Cl-sensor may give an error of 3–10 mM, depending on the background $[Cl]_i$. For more precise estimates, independent measurements of pH_i are necessary to determine the magnitude of pH-dependent modulation of Cl-sensor fluorescence.

Our preliminary analysis demonstrates that Cl-sensor can be successfully used for monitoring changes in $[Cl]_i$ following activation of Cl-selective ion channels and for non-invasive monitoring in different cell types. Particularly promising is using an electroporation protocol for expressing Cl-sensor in living animals. Electroporated retinal cells in rat perfectly express fluorescent proteins for several weeks after electroporation (Matsuda and Cepko, 2004; our observations). This allowed us to estimate $[Cl]_i$ in photoreceptor cells and its changes with K^+-induced depolarization.

The $[Cl]_i$ in retinal cells widely varies depending on the age, type of cell and even dendritic or axonal compartmentalization (Billups and Attwell, 2002; Duebel et al., 2006; Satoh et al., 2001; Zhang et al., 2006). Thus Zhang et al. (2006), using 6-methoxy-*N*-ethylquinolinium iodide (MEQ) for optical measurements of $[Cl]_i$ and perforated-patch recordings for estimation of E_{Cl}, showed that in ganglion and amacrine cells of mouse retina the $[Cl]_i$ shifted from 29 to 14 mM at the time of postnatal development around P6. The study suggests that amacrine and ganglion cells have similar profiles of Cl concentration.

In bipolar cells the difference in the level of $[Cl]_i$ among cell subtypes and even in different compartments of one cell was demonstrated. Using ratiometric two-photon imaging of transgenically expressed Cl indicator, it has been shown that in some bipolar cells of adult mice $[Cl]_i$ in dendrites is up to 20 mM higher than in the soma (Duebel et al., 2006). In another study, using perforated patch-clamp recording from bipolar cells in retina slices from adult rats, the authors also observed differences, albeit much less pronounced; only 4 mM (25 mM and 21 mM in dendrites and at the soma, respectively) (Billups and Attwell, 2002). This higher $[Cl]_i$ in dendrites may result from different distributions of Cl transporters in ON and OFF bipolar cells. NKCC1, which accumulates Cl (rev. Delpire, 2000; Russell, 2000), is expressed in dendrites of rod and cone ON bipolar cells, while KCC2, which extrudes Cl, is expressed in dendrites of cone OFF bipolar cells (Vardi et al., 2000). In line with these observations, a remarkable difference in $[Cl]_i$ between rod and cone bipolar cells was observed. Satoh et al. (2001) estimated that in the retina of adult mouse (6–8 weeks old) the average $[Cl]_i$ was 23.4 mM in the rod bipolar cells, 12.6 mM in the ON-type cone and 7.9 mM in the OFF-type cone bipolar cells.

The chloride concentration in photoreceptors is relatively high. For instance, in salamander cones and rods the chloride equilibrium potentials (E_{Cl}) are about −45 mV and −20 mV, respectively (Thoreson and Bryson, 2004; Thoreson et al., 2002). This corresponds to a range of $[Cl]_i$ from 20 mM to more than 50 mM. Our data show that the mean $[Cl]_i$ in juvenile photoreceptor cells is above 30 mM; this corresponds to a mean E_{Cl} of about −40 mV. While systematic analysis will be necessary to analyse the distribution of $[Cl]_i$ in different photoreceptor subtypes these observations suggests that, similarly to salamander, the $[Cl]_i$ in photoreceptors of rat is high and E_{Cl} is, presumably, close to or slightly more positive than the dark resting potential. As one physiological consequence, this suggests that activation of Cl-selective channels would tend to stabilize the cell membrane potential near the dark potential (Thoreson and Bryson, 2004).

Altogether, our results demonstrate that Cl-sensor possesses relatively high sensitivity to Cl and allows to non-invasive analysis of the distribution of intracellular Cl concentration in different areas of brain and in some other tissues at different conditions.

Development of transgenic animals expressing Cl-sensor will be particularly useful for studies of inhibitory neuronal networks in brain slice preparations using two-photon microscopy. This probe promises to be useful for screening pharmacological agents in the treatment of disorders involving inhibitory neurotransmission.

Acknowledgements

We wish to thank Dr. I. Medina for his help with some experiments and critical reading of the manuscript. We thank also Dr. A. Ivanov and C. Pellegrino for their help with some cultures, and Dr. G. Haase for BTX electroporator. This work was supported by a Fellowship from the French Ministry of Foreign Affairs for O.M. and by French Association against Myopathies (AFM) for M.M.

Appendix A. Supplementary data

Supplementary data associated with this article can be found, in the online version, at doi:10.1016/j.jneumeth.2007.12.016.

References

Ashcroft FM. Ion channels and disease. Academic Press; 2000.

Aslanova UF, Morimoto T, Farajov EI, Kumagai N, Nishino M, Sugawara N, et al. Chloride-dependent intracellular pH regulation via extracellular calcium-sensing receptor in the medullary thick ascending limb of the mouse kidney. Tohoku J Exp Med 2006;210:291–300.

Billups D, Attwell D. Control of intracellular chloride concentration and GABA response polarity in rat retinal ON bipolar cells. J Physiol 2002;545: 183–98.

Biwersi J, Verkman AS. Cell-permeable fluorescent indicator for cytosolic chloride. Biochemistry 1991;30:7879–83.

Bormann J, Hamill OP, Sakmann B. Mechanism of anion permeation through channels gated by glycine and gamma-aminobutyric acid in mouse cultured spinal neurones. J Physiol 1987;385:243–86.

Chesler M. Regulation and modulation of pH in the brain. Physiol Rev 2003;83:1183–221.

Chub N, Mentis GZ, O'donovan MJ. Chloride-sensitive MEQ fluorescence in chick embryo motoneurons following manipulations of chloride and during spontaneous network activity. J Neurophysiol 2006;95:323–30.

Deitmer JW, Rose CR. pH Regulation and proton signalling by glial cells. Prog Neurobiol 1996;48:73–103.

Delpire E. Cation-chloride cotransporters in neuronal communication. News Physiol Sci 2000;15:309–12.

Demaurex N, Frieden M. Measurements of the free luminal ER Ca(2+) concentration with targeted "cameleon" fluorescent proteins. Cell Calcium 2003;34:109–19.

Djamgoz MB, Laming PJ. Micro-electrode measurements and functional aspects of chloride activity in cyprinid fish retina: extracellular activity and intracellular activities of L-type and C-type horizontal cells. Vision Res 1987;27:1481–9.

Duebel J, Haverkamp S, Schleich W, Feng G, Augustine GJ, Kuner T, et al. Two-photon imaging reveals somatodendritic chloride gradient in retinal ON-type bipolar cells expressing the biosensor Clomeleon. Neuron 2006;49:81–94.

Elsliger MA, Wachter RM, Hanson GT, Kallio K, Remington SJ. Structural and spectral response of green fluorescent protein variants to changes in pH. Biochemistry 1999;38:5296–301.

Fucile S, De Saint Jan D, de Carvalho LP, Bregestovski P. Fast potentiation of glycine receptor channels of intracellular calcium in neurons and transfected cells. Neuron 2000;28:571–83.

Galietta LJ, Haggie PM, Verkman AS. Green fluorescent protein-based halide indicators with improved chloride and iodide affinities. FEBS Lett 2001a;499:220–4.

Galietta LV, Jayaraman S, Verkman AS. Cell-based assay for high-throughput quantitative screening of CFTR chloride transport agonists. Am J Physiol Cell Physiol 2001b;281:C1734–42.

Gandhi CS, Loots E, Isacoff EY. Reconstructing voltage sensor-pore interaction from a fluorescence scan of a voltage-gated K+ channel. Neuron 2000;27:585–95.

Gorostiza P, Volgraf M, Numano R, Szobota S, Trauner D, Isacoff EY. Mechanisms of photoswitch conjugation and light activation of an ionotropic glutamate receptor. Proc Natl Acad Sci USA 2007;104:10865–70.

Hamill OP, Bormann J, Sakmann B. Activation of multiple-conductance state chloride channels in spinal neurones by glycine and GABA. Nature 1983;305:805–8.

Haverkamp S, Wassle H, Duebel J, Kuner T, Augustine GJ, Feng G, et al. The primordial, blue-cone color system of the mouse retina. J Neurosci 2005;25:5438–45.

Inglefield JR, Schwartz-Bloom RD. Confocal imaging of intracellular chloride in living brain slices: measurement of GABAA receptor activity. J Neurosci Method 1997;75:127–35.

Ivanov A, Pellegrino C, Rama S, Dumalska I, Salyha Y, Ben-Ari Y, et al. Opposing role of synaptic and extrasynaptic NMDA receptors in regulation of the extracellular signal-regulated kinases (ERK) activity in cultured rat hippocampal neurons. J Physiol 2006;572:789–98.

Jayaraman S, Biwersi J, Verkman AS. Synthesis and characterization of dual-wavelength Cl-sensitive fluorescent indicators for ratio imaging. Am J Physiol 1999;276:C747–57.

Jayaraman S, Haggie P, Wachter RM, Remington SJ, Verkman AS. Mechanism and cellular applications of a green fluorescent protein-based halide sensor. J Biol Chem 2000;275:6047–50.

Khalilov I, Holmes GL, Ben-Ari Y. In vitro formation of a secondary epileptogenic mirror focus by interhippocampal propagation of seizures. Nat Neurosci 2003;6:1079–85.

Kneen M, Farinas J, Li Y, Verkman AS. Green fluorescent protein as a noninvasive intracellular pH indicator. Biophys J 1998;74:1591–9.

Krapf R, Berry CA, Verkman AS. Estimation of intracellular chloride activity in isolated perfused rabbit proximal convoluted tubules using a fluorescent indicator. Biophys J 1988;53:955–62.

Kruger W, Gilbert D, Hawthorne R, Hryciw DH, Frings S, Poronnik P, et al. A yellow fluorescent protein-based assay for high-throughput screening of glycine and GABAA receptor chloride channels. Neurosci Lett 2005;380:340–5.

Kuner T, Augustine GJ. A genetically encoded ratiometric indicator for chloride: capturing chloride transients in cultured hippocampal neurons. Neuron 2000;27:447–59.

Lerche H, Weber YG, Jurkat-Rott K, Lehmann-Horn F. Ion channel defects in idiopathic epilepsies. Curr Pharm Des 2005;11:2737–52.

Llopis J, McCaffery JM, Miyawaki A, Farquhar MG, Tsien RY. Measurement of cytosolic, mitochondrial, and Golgi pH in single living cells with green fluorescent proteins. Proc Natl Acad Sci USA 1998;95:6803–8.

Mansoura MK, Biwersi J, Ashlock MA, Verkman AS. Fluorescent chloride indicators to assess the efficacy of CFTR cDNA delivery. Hum Gene Ther 1999;10:861–75.

Marandi N, Konnerth A, Garaschuk O. Two-photon chloride imaging in neurons of brain slices. Pflugers Arch 2002;445:357–65.

Matsuda T, Cepko CL. Electroporation and RNA interference in the rodent retina in vivo and in vitro. Proc Natl Acad Sci USA 2004;101:16–22.

Metzger F, Repunte-Canonigo V, Matsushita S, Akemann W, ez-Garcia J, Ho CS, et al. Transgenic mice expressing a pH and Cl-sensing yellow-fluorescent protein under the control of a potassium channel promoter. Eur J Neurosci 2002;15:40–50.

Miyawaki A. Fluorescence imaging of physiological activity in complex systems using GFP-based probes. Curr Opin Neurobiol 2003;13:591–6.

Muanprasat C, Kaewmokul S, Chatsudthipong V. Identification of new small molecule inhibitors of cystic fibrosis transmembrane conductance regulator protein: in vitro and in vivo studies. Biol Pharm Bull 2007;30: 502–7.

Myers VB, Haydon DA. Ion transfer across lipid membranes in the presence of gramicidin A. II The ion selectivity. Biochim Biophys Acta 1972;274:313–22.

Nakamura T, Kaneko H, Nishida N. Direct measurement of the chloride concentration in newt olfactory receptors with the fluorescent probe. Neurosci Lett 1997;237:5–8.

Neild TO, Thomas RC. Intracellular chloride activity and the effects of acetylcholine in snail neurones. J Physiol 1974;242:453–70.

Ozawa T, Saito Y, Nishiyama A. Mechanism of uphill chloride transport of the mouse lacrimal acinar cells: studies with Cl-sensitive microelectrode. Pflugers Arch 1988;412:509–15.

Painter RG, Wang G. Direct measurement of free chloride concentrations in the phagolysosomes of human neutrophils. Anal Chem 2006;78:3133–7.

Pasantes-Morales H, Lezama RA, Ramos-Mandujano G, Tuz KL. Mechanisms of cell volume regulation in hypo-osmolality. Am J Med 2006;119:S4–11.

Pedemonte N, Diena T, Caci E, Nieddu E, Mazzei M, Ravazzolo R, et al. Antihypertensive 1,4-dihydropyridines as correctors of the cystic fibrosis transmembrane conductance regulator channel gating defect caused by cystic fibrosis mutations. Mol Pharmacol 2005;68:1736–46.

Rhoden KJ, Cianchetta S, Stivani V, Portulano C, Galietta LJ, Romeo G. Cell-based imaging of sodium iodide symporter activity with the yellow fluorescent protein variant YFP-H148Q/I152L. Am J Physiol Cell Physiol 2007;292:C814–23.

Rohrbough J, Spitzer NC. Regulation of intracellular Cl- levels by Na(+)-dependent Cl- cotransport distinguishes depolarizing from hyperpolarizing GABAA receptor-mediated responses in spinal neurons. J Neurosci 1996;16:82–91.

Russell JM. Sodium–potassium–chloride cotransport. Physiol Rev 2000;80: 211–76.

Satoh H, Kaneda M, Kaneko A. Intracellular chloride concentration is higher in rod bipolar cells than in cone bipolar cells of the mouse retina. Neurosci Lett 2001;310:161–4.

Schwartz RD, Yu X. Optical imaging of intracellular chloride in living brain slices. J Neurosci Method 1995;62:185–92.

Siegel MS, Isacoff EY. A genetically encoded optical probe of membrane voltage. Neuron 1997;19:735–41.

Slemmer JE, Matsushita S, De Zeeuw CI, Weber JT, Knopfel T. Glutamate-induced elevations in intracellular chloride concentration in hippocampal cell cultures derived from EYFP-expressing mice. Eur J Neurosci 2004;19:2915–22.

Suzuki M, Morita T, Iwamoto T. Diversity of Cl(−) channels. Cell Mol Life Sci 2006;63:12–24.

Thoreson WB, Bryson EJ. Chloride equilibrium potential in salamander cones. BMC Neurosci 2004;5:53.

Thoreson WB, Stella Jr SL, Bryson EI, Clements J, Witkovsky P. D2-like dopamine receptors promote interactions between calcium and chloride channels that diminish rod synaptic transfer in the salamander retina. Vis Neurosci 2002;19:235–47.

Trapp S, Luckermann M, Brooks PA, Ballanyi K. Acidosis of rat dorsal vagal neurons in situ during spontaneous and evoked activity. J Physiol 1996;496(Pt 3):695–710.

Tyzio R, Cossart R, Khalilov I, Minlebaev M, Hubner CA, Represa A, et al. Maternal oxytocin triggers a transient inhibitory switch in GABA signaling in the fetal brain during delivery. Science 2006;314:1788–92.

Vardi N, Zhang LL, Payne JA, Sterling P. Evidence that different cation chloride cotransporters in retinal neurons allow opposite responses to GABA. J Neurosci 2000;20:7657–63.

Verkman AS. Development and biological applications of chloride-sensitive fluorescent indicators. Am J Physiol 1990;259:C375–88.

Wachter RM, Remington SJ. Sensitivity of the yellow variant of green fluorescent protein to halides and nitrate. Curr Biol 1999;9:R628–9.

Wachter RM, Yarbrough D, Kallio K, Remington SJ. Crystallographic and energetic analysis of binding of selected anions to the yellow variants of green fluorescent protein. J Mol Biol 2000;301:157–71.

Willoughby D, Schwiening CJ. Electrically evoked dendritic pH transients in rat cerebellar Purkinje cells. J Physiol 2002;544:487–99.

Yang H, Shelat AA, Guy RK, Gopinath VS, Ma T, Du K, et al. Nanomolar affinity small molecule correctors of defective Delta F508-CFTR chloride channel gating. J Biol Chem 2003;278:35079–85.

Zhang LL, Pathak HR, Coulter DA, Freed MA, Vardi N. Shift of intracellular chloride concentration in ganglion and amacrine cells of developing mouse retina. J Neurophysiol 2006;95:2404–16.